Characterizing Closure Asperities by Ultrasonic Measurements

R. B. THOMPSON, L. VAN WYK, D. K. REHBEIN, Y. -M. TSAI and O. BUCK

Ames Laboratory and Departments of Materials Science and Engineering and Engineering Science & Mechanics, Iowa State University, Ames, Iowa 50011, USA

ABSTRACT

It has recently been shown that considerable information about the topology of contacting asperities on the faces of fatigue cracks can be obtained from ultrasonic measurements. The particular configuration of interest is that of a fatigue crack in a compact tension specimen, illuminated at normal incidence by a longitudinal elastic wave. Previous work has suggested that the number density and dimensions of the contacts can be deduced from measurements of the frequency and spatial variations of the scattered elastic wave fields. This paper uses an analysis of the spatial Fourier transform of the dynamic crack opening displacement to interpret those conclusions and analyze several recent experimental results.

KEYWORDS

Acoustic scattering; asperitis; crack tip shielding; diffraction; quasi-static spring model; through transmission.

INTRODUCTION

The growth of a fatigue crack is generally modeled in terms of empirical rules such as the Paris Law (Paris and Erdogan, 1963), which states that $da/dn = A(\Delta K)^m$ where a is the crack length, n is the number of fatigue cycles at a stress intensity range ΔK, and A and m are material constants. Over the last decade, a mounting body of evidence has established that the full excursion of the applied load does not drive the crack tip forward due to a variety of phenomena which are often referred to as crack tip shielding (Ritchie, 1988). In one class of shielding, contact is assumed to develop along the crack faces at plastically deformed asperities, dislodged oxide particles or other geometrical features which prevent a perfect mating of the fracture surfaces when the applied load is released. Since these contacts bear load, they modify the stresses acting at the tip, thereby altering the crack growth rate. This influence of contacting asperities on crack growth rate is discussed in a companion paper (Buck et al., 1989). The present paper addresses the problem of experimentally characterizing the

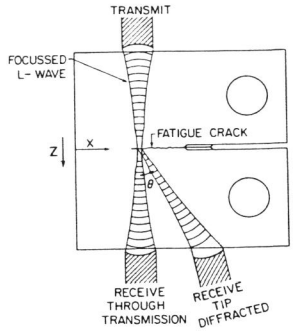

Fig. 1. Experimental configuration.

topology of contact. As discussed below, ultrasonic scattering measurements have been found to be able to provide considerable information towards this end.

EXPERIMENTAL CONFIGURATION

The experimental configuration for the ultrasonic measurements is shown in Fig. 1. A fatigue crack, grown in a compact tension specimen, is illuminated by a longitudinal wave incident perpendicular to the crack face and focused in the plane of the crack. The longitudinal wave transmitted directly past the crack can be picked up by a coaxial receiver placed on the opposite side of the specimen. Alternatively, by changing the angular orientation of the receiver and translating it so that it is still directed towards the illuminated spot, longitudinal or transverse waves diffracted from the crack tip or contacting asperities are detected. Differentiation of the diffracted L and T waves is aided by their different times of arrival.

By comparing these signals to those observed in a reference experiment in which the beam is directly transmitted through the uncracked ligament, most of the influence of the measurement system, such as the efficiency of the transducers, is eliminated from the data. This deconvolved information is thus characteristic of the crack itself. By spectral analysis, translation of the sample, or rotation of the receiver, one can respectively monitor the frequency, spatial, and angular dependence of the crack transmissivity.

THEORY OF THE MEASUREMENT

General Considerations

In order to interpret this complex information, a unifying theory is required. Based on the electromechanical reciprocity relation of Auld (1979), it has recently been shown that the received electrical signal is given by (Thompson et al., 1987)

$$\Gamma \cong \frac{j\omega}{4P} \int_{A+} (2u_i^I - \Delta u_i^T)\, \tau_{ij}^R\, n_j^+\, dA \qquad (1)$$

where Γ is the electrical signal transmitted from the transmitting to the receiving transducer, ω is the angular frequency, P is the electrical power

incident on the transmitting probe, u_i^I is the dynamic displacement field that would be produced in the crack plane by the transmitting probe had the crack been absent, Δu_i^T is the dynamic crack-opening displacement (DCOD) of the crack faces as driven by these fields, τ_{ij}^R is the dynamic field that would be produced in an uncracked sample had the receiver been excited by the electrical power P, and n_j^+ is the normal to the crack face.

The predictions of Eq. (1) depend on the characteristics of the transducer radiation through the dependence of $\vec{u}$ and $\vec{\tau}$ on the incident electrical power P. It is useful to assume that the illuminating longitudinal wave displacement field only has a 3-component and to assume the existence of a normalized DCOD defined by the relation

$$\Delta\xi_i = \Delta u_i^T / u_3^I. \qquad (2)$$

Equations (1) and (2) then combine to give

$$\Gamma \cong \frac{j\omega}{4P} \int_{A+} (2\delta_{3i} - \Delta\xi_i)\, u_3^I\, \tau_{i3}^R\, dA \qquad (3)$$

where δ_{3i} is the Kronecker delta.

In the plane of the crack, one may also write

$$u_3^I = A^I(\omega, \vec{R} - \hat{R}), \quad \tau_{i3}^R = A_i^R(\omega, \theta, \vec{R}-\hat{R}) e^{-jk(x-\hat{x})\sin\theta} \qquad (4)$$

where A^I and A_i^R are beam profiles, $\vec{R}$ is a coordinate vector in the crack plane, and k is the wave vector of the polarization detected by the receiver. The "^" denotes the coordinates of the common intersection of the beam axes. If one defines $B(\omega,\theta,\vec{R}-\hat{R})$ to be the product $A^I A_i^R$, then Eqs. (3) and (4) combine to yield

$$\Gamma(\omega,\theta,\hat{R}) \cong \frac{j\omega}{4P} \int_{-\infty}^{\infty} dx \int_{-\infty}^{\infty} dy\; B(\omega,\theta,\vec{R}-\hat{R})\left[2\delta_{3i} - \Delta\xi_i(\vec{R})\right] e^{-jk(x-\hat{x})\sin\theta} \qquad (5)$$

Equation (5) is a summation over the three components of the DCOD. For simplicity, only the contributions of the 3-component, which is expected to be dominant, will be considered in the remainder of this paper.

There are three independent variables, θ, $\hat{x}$ and $k = 2\pi f/v$ which can be varied in an experiment. The goal is to use this information to gain information on $\overrightarrow{\Delta\xi}(\vec{R})$, i.e. on the contact topology which shields applied load excursions from the crack tip. In principle, one could devise calibration experiments to determine B. Then by measuring the received signal as a function of k and/or θ, followed by similar experiments in which the receiver was tilted in the y-direction, one could define the spatial Fourier transform of $\overrightarrow{\Delta\xi}$ and then reconstruct its detailed form by evaluation of the inverse transform. In practice, however, this is not possible because a) it is difficult to experimentally obtain the phase of the signal with sufficient accuracy due to possible variations in metal path, and b) one cannot readily make measurements at sufficiently high frequencies to resolve the small contact spacings. Therefore, the less elegant procedure of picking parameterized trial forms for $\Delta\xi_3$ and varying the parameters to fit the theory have been employed.

This general formalism will next be applied to some special cases to illustrate the type of information that one can expect to obtain. As a starting point, Fig. 2 sketches the expected spatial variation of several functions

which play a key role in the theory. Part a) shows the DCOD for an ideal crack with no contacting asperities as it rapidly rises from the value of zero at the tip to a value of approximately two on the face. Oscillations about that value, due to Rayleigh waves propagating on the crack face, will be neglected for simplicity. In the Kirchhoff approximation, this DCOD is approximated by a step function as indicated by the dashed line. As shown in part b), the DCOD of a crack with contacting asperities rapidly oscillates between the value of zero at the contacting asperities to a finite value in the intervening regions. Part c) indicates the phase of the local average of the DCOD, which was indicated by a dashed line in part b). The $\pi/2$ shift is dictated by the fact that, within the Kirchhoff approximation, the DCOD will be in phase with the displacement of the incident wave over the contact-free faces of the crack. However, assuming that the contact spacings are much less than a wavelength, the displacement in the cracked portions will tend to follow the stress of the incident wave and thus be shifted by $\pi/2$ from the incident displacement field. Part d) indicates a diffraction limited beam size that is a few wavelength in dimensions. In this paper, it will be assumed that $L>>W>\lambda>>C$ where L is the spatial extent of the closure region, W is the spot size, λ is the wavelength, and C is the contact separation.

Through Transmission

Consider a through transmission measurement, for which $\theta = 180°$ and thus $\sin\theta = 0$. From Eq. (5) and the slow variation of B over the dimensions of the contact separations, it follows that

$$\Gamma(\omega,180°,\hat{R}) = \frac{j\omega}{4P}\int_{-\infty}^{\infty}dx\int_{-\infty}^{\infty}dy\ B(\omega,180°,R-\hat{R})\left[2-\overline{\Delta\xi_3}(\vec{R})\right] \qquad (6)$$

where $\overline{\Delta\xi_3}(\vec{R})$ is the local average of the DCOD. The integral of the first term in brackets is equal to the result of the reference experiment, and hence contributes unity to the deconvolved result. The second term

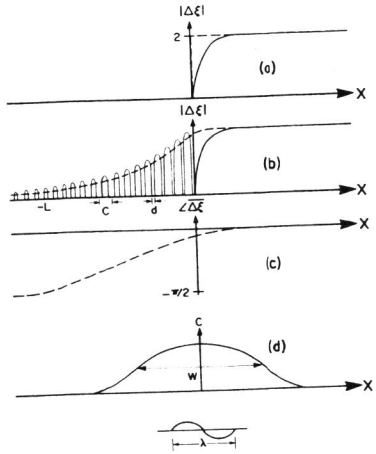

Fig. 2.

Schematic spatial variations of
a. DCOD for "ideal" crack.
b. DCOD for crack with contacting asperities.
c. Phase of local average DCOD for crack with contacting asperities.
d. Beam overlap function.

thus describes the crack induced decrease in transmission. The contribution of the second term to the integrand is sketched for several values of $\hat{x}$ in Fig. 3. The solid line indicates the results for the ideal crack, as modeled by the Kirchhoff approximated. The dashed line indicates that of a crack with asperities. The gradual decrease in transmission as $\hat{x}$ increases is also shown.

To allow this behavior to be quantified, a model for $\overline{\Delta\xi_3}$ has been developed based on quasi-static arguments. When there are many contacts per wavelength, it is assumed that $\overline{\Delta u_3}^T = \sigma/\kappa$ where σ is the stress existing at the interface during the wave interaction. Furthermore, it is assumed that κ can be related to the topology of the interface using standard elasticity solutions for static crack deformation (Baik and Thompson, 1984). One then concludes

$$\Gamma(\omega,180°,\hat{R}) = \frac{j\omega}{2P}\int dx\int dy\ \left[1+j\alpha(\vec{R})\right]^{-1}B(\omega,180°,\vec{R}-\hat{R}) \qquad (7)$$

where $\alpha(\vec{R}) = \pi\rho vf/\kappa(\vec{R})$. By postulating various functional forms for κ, one can attempt to fit $\Gamma(\omega,180°,\hat{R})$ to experimental data. If a successful fit can be obtained, one has experimentally determined the "spring constant" or crack stiffness which results from the contacting asperities.

This procedure provides important information on the topology of contact. However, it is not complete, as can be seen from explicit expression for κ. For examples for non-interacting contacts, κ determines the product dN, where d is the contact diameter and N is their number density. Since dN is not the parameter controlling crack tip shielding, additional information is needed to fully define the crack contact topology to the extent needed to predict modifications in crack growth rates.

Tip Diffraction

When θ is changed from 180°, one is describing the signal diffracted from the crack tip. In general, experiments are set up in such a way that the signal in the uncracked ligament is of negligible amplitude. The formula predicting the behavior for this scattered field may be obtained by dropping the term $2\delta_{3j}$ in Eq. (5). As noted before, this is a Fourier transform of the DCOD, modulated by the beam profile.

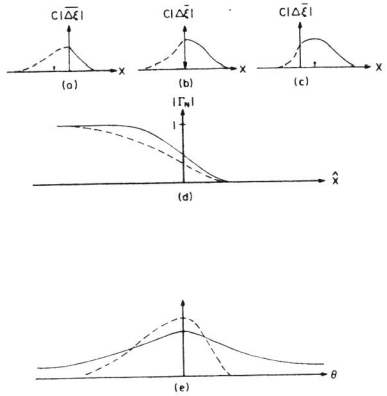

Fig. 3.

Schematic spatial variations of
a. $B|\overline{\Delta\xi_3}|$ for $\hat{x} < 0$.
b. $B|\overline{\Delta\xi_3})|$ for $\hat{x} = 0$.
c. $B|\overline{\Delta\xi_3}|$ for $\hat{x} > 0$.
d. $|\Gamma^N(\omega,180°,\hat{R})|$.
e. $|\Gamma^N(\omega,\theta,0)|$.
Solid lines: ideal crack.
Dashed lines: closure described by locally averaged DCOD.

Consider first the ideal crack. In the Kirchhoff approximation, the integrand has the same general form as in Fig. 3b, although it may differ slightly due to the variation of beam width with angle of incidence. Fig. 3e illustrates the Fourier transform of that function, plotted as a function of $p = k\sin\theta$. The slow decrease in diffracted signal with angle is a consequence of the high spatial frequencies present in the Fourier transform of a step function. When partial closure is present and the quasi-static spring model is used to model the DCOD, as indicated by the dashed line, the sharp singularity, and high spatial frequencies, of the ideal DCOD vanish. Consequently, the predicted scattering at higher angles is greatly reduced. Moreover, the Fourier transform is somewhat asymmetric due to the phase variation of $\overline{\Delta\xi_3}$.

However, comparison of this model to experiment has revealed that the predictions are much lower than the measurements. It has been proposed that the problem is associated with the absence of discrete contacts in the model (Rebhein et al., 1985). To interpret this in terms of the theory of Fourier transforms, suppose that one can write $\Delta\xi_3(x) = \overline{\Delta\xi}_3(x)\ M(x)$ where $M(x)$ is a rapidly varying modulation, with zero mean. Using the symbol F to denote the Fourier transform operation

$$F[\Delta\xi_3(x)] = F[\overline{\Delta\xi}_3(x)]*F[M(x)] \qquad (8)$$

where * denotes convolution. Rapid oscillations in M lead to much greater energy in the high spatial frequencies of the Fourier transform of $\Delta\xi_3$ than in that of $\overline{\Delta\xi}_3$. It is these components that the theory predicts are detected in a diffraction experiment. When M is replaced by a periodic series of delta functions, specific calculations have been carried out. These show that the magnitude of the tip diffracted signal is very sensitive to the number density of contacts and this sensitivity has been used as a basis of the estimate of that density.[7] In this delta function approximation, $F(\Delta\xi_3(x))$ becomes a series of replicas of $F(\overline{\Delta\xi}_3)$, centered at $p = 2\pi n/C$, where C is the contact separation. Note that the asymmetry of $F(\Delta\xi_3)$ can lead to a greater contribution to the diffracted signal from the spectrum centered at $p = 2\pi/C$ than from that centered at $p = 0$. However, as $C \to 0$, these discrete contributions ultimately become spread out and the response is dominated by the central replica of $F(\Delta\xi_3)$. In this limit, the predictions of the delta function model approach those of the quasi-static spring model.

EXPERIMENTAL RESULTS

Ideal Crack

Figure 4 compares theory and experiment for an "ideal crack," simulated by a saw slot. Transmitted signals have been previously reported by Thompson et al. (1984). Here, the diffracted shear waves are shown. Part a) shows the angular dependence of the diffracted shear wave at discrete frequencies. The corresponding theoretical results are shown in part b). There is good qualitative agreement between the two results, although the theory tends to decrease in magnitude somewhat more rapidly with frequency. The observed responses are a product of two factors. The wave-crack interaction produces a response which gradually rolls off with angle, as shown in Fig. 3e. However, the liquid-solid interface transmission coefficient has considerable structure which strongly influences the diffracted magnitude.

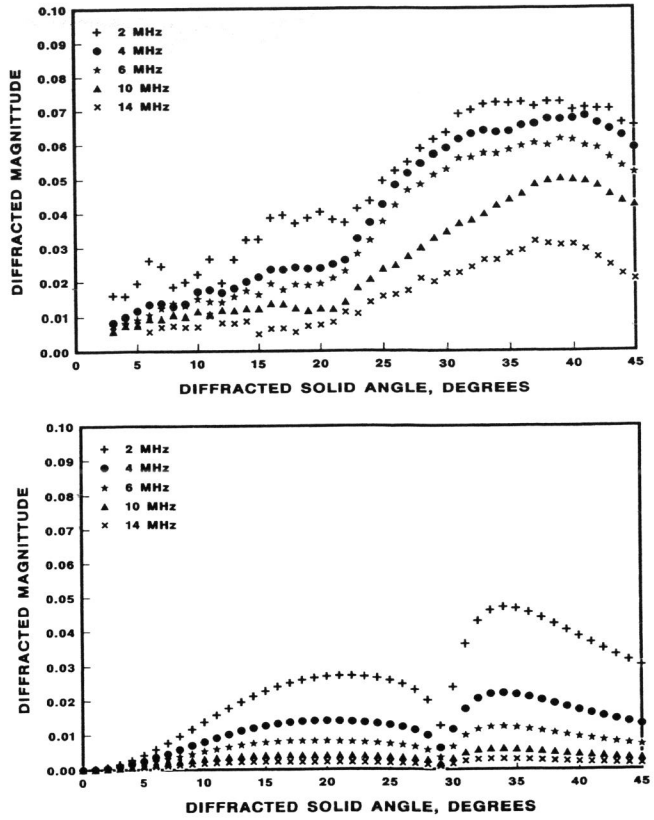

Fig. 4. Shear wave diffraction from saw slot simulating ideal crack. a. Experiment, b. Theory.

Simulated Fatigue Crack

In order to simulate a partially contacting crack with known contact topology, a screen-like mesh of disbonds was induced in an iron sample by powder metallurgical techniques (Hsu and Thompson, 1988). The resulting dependence of the transmitted signal on position is shown in Fig. 5a. Theoretical predictions for the response of this "crack" are shown in Fig. 5b, using the spring model, Eq. (7). Here the spring constant was chosen to have a value of $\kappa = 1.17 \times 10^{12}$ dynes/cm^3 over the face of the crack, and $\kappa = \infty$ (perfect contact) in the uncracked ligament. Theory and experiment agree well for frequencies up to 6 MHz. At higher frequencies the signal tends to drop more rapidly in experiment than in theory. Other measurements have shown this to be a consequence of significant energy being scattered in other than the forward and backward directions, thus violating an assumption used in deriving the quasi-static spring model.

Scattering from Fatigue Cracks

A number of experiments have been performed on fatigue cracks, leading to several new observations regarding the crack closure phenomenon. Here, three recent conclusions are summarized.

(a)

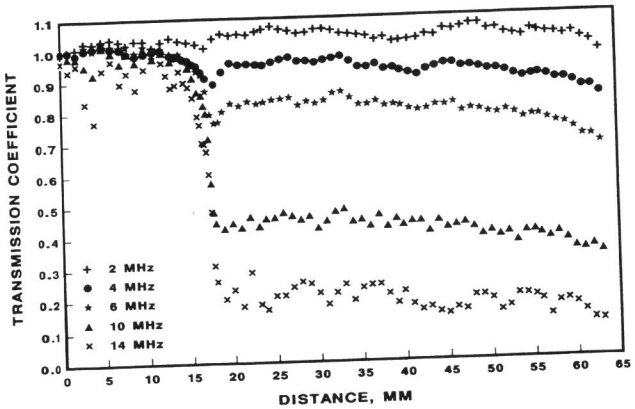

Fig. 5.

Transmission through gridded iron sample. a. Experiment, b. Theory.

(b)

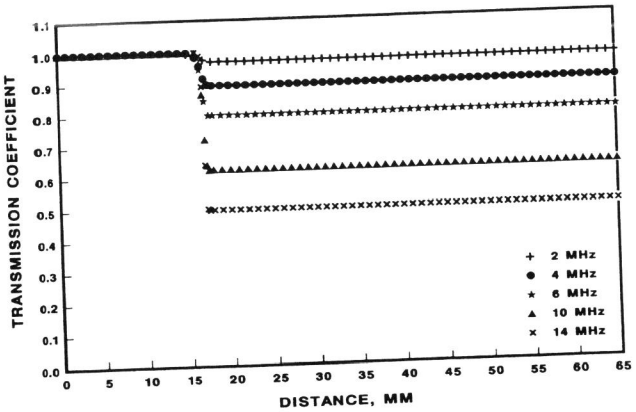

Extent of Closure Zone. Measurements of the through transmission data, for a fatigue crack grown in Al 7075-T651 showed a large spatial extent of the closure (Buck et al., 1988), comparable to that implied by x-ray stress measurements (Welsch et al., (1987), but much greater than would have been expected based on some previous models of crack closure phenomena.

Effect of Overloads. It is well known that a single cycle or block of overload pulses during the growth of a fatigue crack will retard its growth. Previous ultrasonic measurements have shown that the overload produces a region of enhanced asperity contact which persists even after subsequent cycling of sufficient extent to cause the crack to reinitiate (Rehbein et al., 1988). More recent measurements have been made directly after the application of the overload. The effects of discrete contacts are not seen in this data, which is consistent with the concept of massive closure which holds the crack faces in virtually complete contact.

Effects of Growth under Decreasing ΔK. Load shedding crack growth studies are made for a variety of reasons, including the study of initiation

effects. In that case, it is argued that crack growth rate will decrease as the load is decreased until the threshold for initiation is reached. Ultrasonic measurements made on such specimens have shown an extensive region of closure along the crack wake (Rehbein et al., 1988). At any frequency, the data look quite similar to those obtained on the constant grid mesh shown in Fig. 5. However, in contrast to those results, the signals do not fall off rapidly with frequency, implying that the spring model is not applicable. One possible explanation suggested by the analysis presented in this paper is that the contact dimensions and separations are considerably greater. These samples have a very large component of diffracted shear waves in the near forward direction (Rehbein et al., 1988) which is also consistent with this interpretation.

CONCLUSIONS

It has been shown that ultrasonic measurements provide important information on the degree of contact across the faces of a fatigue crack and hence on the degree of shielding of the tip from excursion in the applied load. Fourier transform analysis is used to illustrate the theory and clarify the dependence of through transmitted and tip diffracted signals on the contact topology. The theory is used to interpret a series of experiments on samples ranging from saw slots, grids with controlled constant dimensions, and fatigue cracks grown under a variety of conditions. The implication of this data on crack growth rate is discussed in a companion paper (Buck et al., 1989).

A variety of crack-tip shielding mechanisms are being utilized in attempts to increase the toughness of ceramics. For example, ligament bridging can shield the tip of the crack from the full excursions of the applied load (Cook et al., 1987). It is suggested that the above ultrasonic techniques could be adapted to provide important new information in the study of those phenomena.

ACKNOWLEDGMENT

Ames Laboratory is operated for the U.S. Department of Energy by Iowa State University under contract No. W-7405-ENG-82. This work was supported by the Office of Basic Energy Sciences, Division of Materials Sciences.

REFERENCES

Auld, B. A., (1979). Wave Motion, 1, 3.

Baik, J.-M. and R. B. Thompson (1984). J. Nondestr. Eval., 4, 177.

Buck, O., R. B. Thompson and D. K. Rehbein (1988). In: Mechanics and Physics of Crack Growth: Application to Life Prediction. Materials Science and Engineering, A103, 37.

Buck, O., R. B. Thompson, D. K. Rehbein, L. J. H. Brasche and D. D. Palmer (1989). This proceedings.

Cook, R. F., C. J. Fairbank, B. R. Lawn and Y.-W. Mai (1987). J. Mater. Res., 2, 345.

Hsu, D. K., and D. O. Thompson (1988). In: Review of Progress in Quantitative Nondestructive Evaluation (D. O. Thompson and D. E. Chimenti, eds.) Vol. 7B, p. 1541. Plenum Press, New York and London.

Paris, P. C., and F. J. Erdogan (1963). J. Basic Engrg., Trans. ASME, D85, 528.

Rehbein, D. K., R. B. Thompson and O. Buck (1985). In: Review of Progress in Quantitative Nondestructive Evaluation (D. O. Thompson and D. E. Chimenti, eds.), Vol. 4A, p. 61. Plenum Press, New York and London.
Rehbein, D. K., L. Van Wyk, R. B. Thompson and O. Buck (1988). In: Review of Progress in Quantitative Nondestructive Evaluation (D. O. Thompson and D. E. Chimenti, eds.), Vol. 7B, p. 1301. Plenum Press, New York and London.
Ritchie, R. O. (1988). In: Mechanics and Physics of Crack Growth: Application to Life Prediction. Materials Science and Engineering, A103, 15.
Thompson, R. B., C. J. Fiedler and O. Buck (1984). In: Nondestructive Methods for Material Property Determination (C. O. Ruud and R. E. Green, Jr., eds.), p. 161. Plenum Press, New York and London.
Thompson, R. B., O. Buck and D. K. Rehbein (1987). In: Proceeding of the Tenth U.S. National Congress of Applied Mechanics (J. P. Lamb, ed.), p. 359. ASME, New York.
Welsch, E., D. Eifler, B. Scholtes and E. Macherauch (1987). In: Residual Stresses in Science and Technology (E. Macherauch and V. Hauk, eds.), p. 785. DGM Informationsgesellschaft Verlag, Oberursel, FRG.